Near-field scanning optical microscopy as a simultaneous probe of fields and band structure of photonic crystals: A computational study

Shanhui Fan,[a] Ian Appelbaum, and J. D. Joannopoulos
Department of Physics, Massachusetts Institute of Technology, Cambridge, Massachusetts 02139

(Received 11 January 1999; accepted for publication 29 June 1999)

We demonstrate the feasibility of employing near-field scanning optical microscopy (NSOM) imaging to simultaneously obtain both the eigenfield distribution and the *band-structure* information of a photonic crystal. We introduce the NSOM measurement configuration required and simulate the imaging process, with both the tip and the sample included, using three-dimensional finite-difference time-domain calculations. Both the field-pattern and the frequency–wave-vector relations of photonic crystal eigenmodes are revealed by analyzing simulated images. © *1999 American Institute of Physics.* [S0003-6951(99)02534-6]

Photonic crystals are predicted to have the capability of drastically affecting the dispersion relations, symmetries, and spatial power distributions of electromagnetic modes within their boundaries and thereby provide a new dimension in controlling the flow of light.[1,2] These predictions are being actively tested by experiments. Most of the experiments performed so far probe the band structure by analyzing amplitudes of scattered electromagnetic waves from the crystal. Such measurements do not provide information concerning the field distribution of the eigenmodes. To obtain such information requires resolution far below the diffraction limit, and near-field scanning optical microscopy (NSOM) (Ref. 3) is useful for this purpose. To this date, however, only a small number of NSOM experiments have been attempted on photonic crystal samples,[4–6] none of which directly probe the eigenmodes of the photonic crystal. In this letter, we introduce a NSOM measurement configuration which allows for direct imaging of photonic crystal eigenmodes, and demonstrate the feasibility of employing NSOM to obtain frequency–wave-vector dispersion information of photonic crystals.

We use a three-dimensional finite-difference time-domain (FDTD) program[7] to simulate the NSOM measurement process. Previously, NSOM measurements have been simulated using two-dimensional finite-difference time-domain methods[8] and multiple multipole methods.[9] In comparison, three-dimensional FDTD methods possess the capability of dealing with more complex structures in a more realistic fashion.

The simulated structure consists of a finite photonic crystal slab and a NSOM tip, as shown in Fig. 1. The computational domain contains $140\times550\times140$ Yee cells.[10] Each Yee cell is cubic in shape with an edge length of $0.05a$, where a is the lattice constant of the photonic crystal. The crystal structure is composed of a triangular array of air holes introduced in a Si slab with an index of 3.48, which is appropriate for light with a wavelength equal to 1.55 μm.[11] The air holes have a radius of $0.4a$ and the slab has a thickness of $0.1a$. These structural parameters are chosen to ensure the single-mode nature of the guided modes, and to increase the decaying length of the exponential tail of the guided modes away from the slab. The tip is made of Si (Ref. 12) with a metallic coating[13] that is perfectly conducting. At the narrow end of the tip, the dielectric core has a radius of $0.08a$. The tip is separated from the surface of the slab by a distance of $0.05a$. Periodic boundary conditions are applied at two of the six computational cell boundaries in order to simulate a photonic crystal with large transverse dimension. On all other boundaries, we apply Mur's absorbing boundary condition to eliminate spurious reflection for outgoing electromagnetic waves.[14]

For an operating wavelength at 1.55 μm, we choose the lattice constant a to be equal to 0.56 μm, to ensure that the operating wavelength falls in the first photonic band. In the simulated structure, the dielectric core at the bottom end of the tip has a diameter of 89 nm. The bottom of the tip is placed 28 nm away from the surface of the dielectric slab. These parameters are reasonable for typical NSOM experiments.[3] For operation at a different wavelength, the structural parameters scale proportionally. Since NSOM experiments can be performed in wide ranges of frequencies, we will use dimensionless units in the following discussion.

The band structure of the *infinite* photonic crystal along the $\Gamma-K$ and $\Gamma-M$ directions for TE-like modes is shown in Fig. 2. A detailed discussion of such band structures can be found in Ref. 15. Because of the single-mode nature of the band structure, individual eigenmodes with a definite wave vector can be excited by specifying the oscillation frequency and propagation direction. Measurement of the time-averaged power distribution of such an eigenmode, however, will be periodic with respect to the lattice vector, and hence, will not provide any information about the wave vector k. In order to generate wave-vector information, we deliberately exploit the properties of a *finite* photonic crystal in order to induce interference between $+k$ and $-k$ eigenmodes. For example, to excite a mode along the $\Gamma-K$ direction, we choose the truncation of the crystal to be normal to the K direction. A plane of oscillating dipoles located in the uniform part is then used to excite a guided mode, which strikes upon the truncation in the normal direction.

The time-averaged power densities for two modes along the $\Gamma-K$ and $\Gamma-M$ directions, respectively, are shown in Fig. 3. Both modes are chosen to possess a normalized fre-

[a]Electronic mail: shanhfan@mit.edu

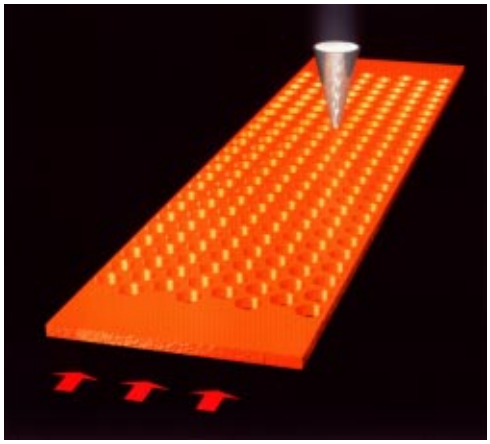

FIG. 1. (Color) The computational cell for the simulation of a near-field optical scanning microscopy measurement process.

quency of 0.36 c/a. The power distribution on a slice located at the top surface of the dielectric structure is plotted. Such a plot represents an unperturbed near-field image in the absence of a tip. It is interesting to note the occurrence of a long-wavelength modulation pattern. For the mode along the $\Gamma-K$ direction, this variation is more clearly displayed on a line graph, as shown in Fig. 4(a). The solid curve represents the power as a function of propagation distance on a line located at the center of the power density image. Inside the photonic crystal, the power is sharply peaked at the positions of the dielectric ribs. In addition, the intensities of the peaks clearly display a long-wavelength envelope modulation with a period roughly equal to five lattice constants.

This long-wavelength modulation is related to the finite extent of the photonic crystal in the simulated structure. The electromagnetic fields in the finite crystal, represented by a generic vector field $\mathbf{F}(\mathbf{r})$, are made up of a linear combination of forward and backward propagating Bloch waves, i.e.,

$$\mathbf{F}(\mathbf{r})=(e^{iky}+be^{-iky})\mathbf{u}(\mathbf{r}), \tag{1}$$

where y is the coordinate along the propagation direction, and b is a complex constant representing the relative amplitude of the backward propagating wave. The function $\mathbf{u}(\mathbf{r})$ is periodic with respect to translations along the lattice vectors of the hexagonal arrays.

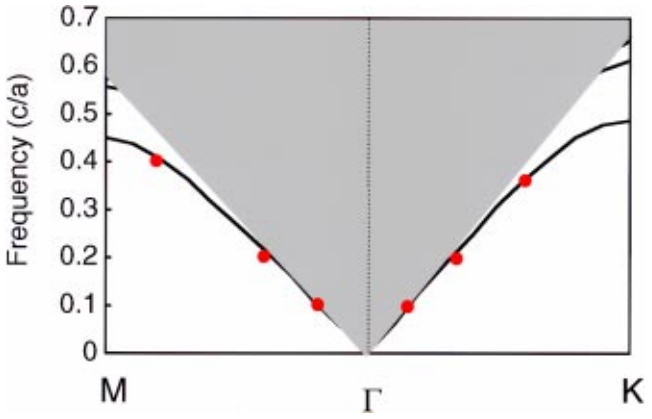

FIG. 2. (Color) Band structure of a photonic crystal slab, possessing a triangular lattice of air holes. The thickness of the slab is $0.1a$ and the radius of the holes is $0.4a$, where a is the lattice constant. Plotted here are modes with TE-like character. The gray region is a continuum of radiation modes. The curves are results from a band-structure calculation, while the solid dots are determined by examining the near-field images.

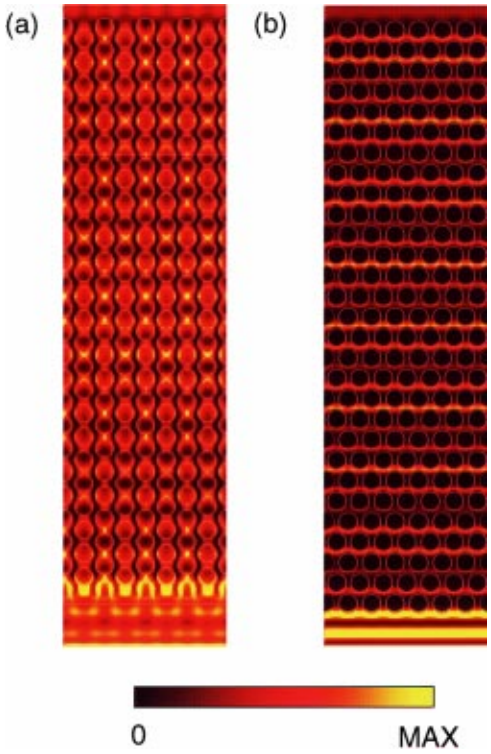

FIG. 3. (Color) Power density distribution on a slice at the surface of the dielectric structure for photonic crystal modes propagating along (a) $\Gamma-K$, and (b) $\Gamma-M$ directions. The mode is excited at a frequency of 0.36 c/a. The circles indicate the positions of the air holes.

The time-averaged power density $P(\mathbf{r})=\mathbf{F}^*(\mathbf{r})\cdot\mathbf{F}(\mathbf{r})$ is, therefore, of the form

$$P(\mathbf{r})=|\mathbf{u}|^2(1+|b|^2)+be^{-2iky}|\mathbf{u}|^2+b^*e^{2iky}|\mathbf{u}|^2. \tag{2}$$

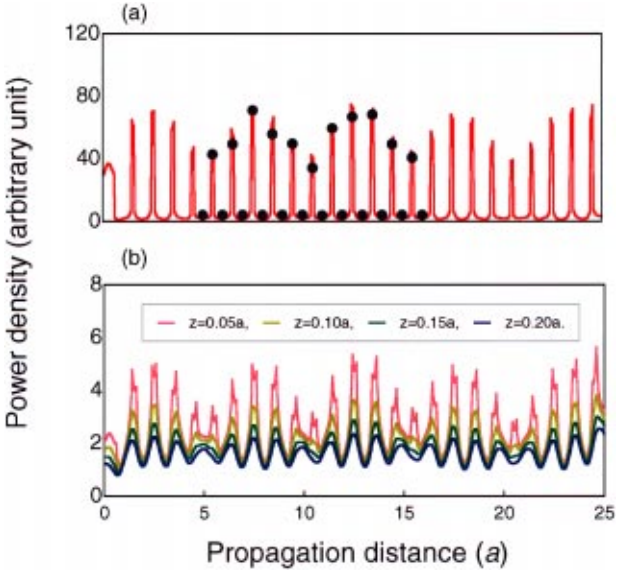

FIG. 4. (Color) (a) Comparison between the power density distribution at the surface of the photonic crystal, and results from NSOM measurement simulations which include both the tip and the sample. The curve represents the power distribution along a line at the center of the image shown in Fig. 3(a), while the dots are results from NSOM measurement simulations. (b) Power density distribution of the photonic crystal mode along a line at different distances z from the surface of the crystal.

TABLE I. Measured flux through the top surface of the tip as a function of tip–sample distance.

Tip–sample distance (a)	Flux (arbitrary units)
0.05	0.044
0.10	0.020
0.15	0.000 29
0.20	0.000 24

The first term on the right-hand side of Eq. (2) displays the same spatial period as the lattice. The second and third terms, on the other hand, can be expanded in terms of Fourier components with the wave-vector set $\{q_y\}$ along the propagation direction determined by

$$\{q_y\}=\{G_y\pm 2k\}, \tag{3}$$

where G_y represents the y component of each reciprocal lattice vector.

In the case where the propagation is along the $\Gamma-K$ direction, the projected reciprocal lattice vectors, i.e., the G_y's, assume the values $m\cdot 2\pi/a$, with m an arbitrary integer. Therefore, with the longest-wavelength modulation at a period of $5a$, [i.e., Fig. 4(a)], we determine the wave vector of the eigenmode to be $0.4\cdot 2\pi/a$,[16] which is to be compared with a band-structure calculation that gives a value of $0.404\cdot 2\pi/a$ at the same frequency. By exciting modes at different frequencies and propagation directions, and analyzing the resulting modulation patterns, we are able to map out a dispersion relation. The results of this analysis for $\Gamma-K$ and $\Gamma-M$ directions are shown as solid dots in Fig. 2. The dispersion relation determined in this way is in excellent agreement with the band-structure calculation.

We now investigate the feasibility of imaging the details of the photonic crystal modal pattern. We first try to establish the required tip–sample distance by analyzing the power density distribution as a function of distance from the sample surface. This is shown in Fig. 4(b). Note that the long-wavelength modulation information decreases much faster than the power density when we move away from the surface of the slab. This is because the photonic crystal modes are made up of more than one in-plane Fourier component, each with different out-of-plane decay lengths. Thus, only in the limit of large separation from the surface will one Fourier component dominate, leading to pure exponential decay of the power density. To be able to capture most of the components it is, therefore, necessary to bring the tip into close proximity of the sample.

Natural questions that immediately arise, therefore, are how strong the tip–sample interaction is, and to what extent meaningful measurements can be made under these conditions. To investigate this, we perform large-scale computer experiments to simulate the essential components of a realistic NSOM measurement process including both the sample and the tip. The computational setup is shown in Fig. 1.

We begin by placing the center of the tip at the position of a peak in the power density and record the flux through the top surface of the tip while varying the tip–sample distance. These results are displayed in Table I. The flux decreases drastically by two orders of magnitude, as we increase the distance from $0.10a$ to $0.15a$. Since, as we have seen in Fig. 4(b), there is no corresponding sudden change in the unperturbed power density, this indicates a strong tip–sample interaction when the distance is smaller than $0.10a$. But as we discussed earlier [Fig. 4(b)], we need to operate within this distance to obtain discernible imaging. To determine whether this strong tip–sample interaction will distort the measured modal pattern, we place the tip at $0.05a$ from the sample, and perform a constant-height scan. The measured results are displayed as solid dots in Fig. 4(a), together with the unperturbed power distribution. The simulated measurements clearly resolve individual peaks in the power distribution. The contrast between measured minima and maxima is at least an order of magnitude. The modulation on the intensity of the peaks is also detected by the simulated measurement, and the measured flux displays the same spatial period as the power distribution. The collection efficiency (the ratio between the measured flux and the input flux per lattice constant) is about 10^{-6}. This is typically detectable under realistic experimental conditions.[17]

Finally, although we have focused for simplicity on a slab geometry with air above and beneath the slab, the same effects should be observable for a photonic crystal guiding layer placed on top of a low-index substrate. In conclusion, these simulations clearly indicate the feasibility of using NSOM to image the eigenfield distribution, and the possibility of using NSOM as a wave-vector spectroscopy tool for band-structure measurements.

This work is supported in part by the MRSEC Program of the NSF under Award No. DMR-9400334. The authors would like to acknowledge discussions with J.W.P. Hsu.

[1] J. D. Joannopoulos, R. D. Meade, and J. N. Winn, *Photonic Crystals: Molding the Flow of Light* (Princeton University Press, Princeton, 1995).
[2] J. D. Joannopoulos, P. R. Villeneuve, and S. Fan, Nature (London) **386**, 143 (1997).
[3] For a review on near-field optical microscopy, see M. A. Paesler and P. J. Moyer, *Near-Field Optics: Theory, Instrumentation and Applications* (Wiley, New York, 1996).
[4] E. B. McDaniel, J. W. P. Hsu, L. S. Goldner, R. J. Tonucci, E. L. Shirley, and G. W. Bryant, Phys. Rev. B **55**, 10878 (1997).
[5] G. H. Vander Rhodes, M. S. Ünlü, B. B. Goldberg, J. M. Pomeroy, and T. F. Krauss, IEE Proc.: Optoelectron. **145**, 379 (1998).
[6] P. L. Philips, J. C. Knight, B. J. Mangan, P. St. J. Russell, M. D. B. Chariton, and G. J. Parker, J. Appl. Phys. **85**, 6337 (1999).
[7] For a review on the finite-difference time-domain method, see K. S. Kunz and R. J. Luebbers, *The Finite Difference Time Domain Method for Electromagnetics* (CRC Boca Raton, FL, 1993)
[8] R. X. Bian, R. C. Dunn, X. S. Xie, and P. T. Leung, Phys. Rev. Lett. **75**, 4772 (1995).
[9] L. Novotny, R. X. Bian, and X. S. Xie, Phys. Rev. Lett. **79**, 645 (1997).
[10] K. S. Yee, IEEE Trans. Antennas Propag. **AP-14**, 302 (1966).
[11] E. D. Palik, *Handbook of Optical Constants of Solids* (Academic, New York, 1985).
[12] We have found a significant increase, by four orders of magnitude, in the amount of power coupled into the tip, when a higher-index material, such as Si, instead of a low-index material, such as SiO_2, is used as the dielectric core.
[13] Our simulations indicate that a coated tip is necessary to prevent coupling of stray light into the tip.
[14] G. Mur, IEEE Trans. Electromagn. Compat. **EMC-23**, 377 (1981).
[15] S. Fan, P. R. Villeneuve, J. D. Joannopoulos, and E. F. Schubert, Phys. Rev. Lett. **78**, 3294 (1997).
[16] Here, we exclude a possible choice of the wave vector $0.1\cdot 2\pi/a$, which would have generated the same set of Fourier components. With the frequency at $0.36c/a$, all guided modes should have a wave vector greater than $0.36\cdot 2\pi/a$.
[17] J. W. P. Hsu (private communications).